Fundamentals of Acoustic Cytometry

Michael D. Ward[1] and Gregory Kaduchak[1]

[1]ThermoFisher Scientific, Eugene, Oregon

Acoustic cytometry uses radiation pressure forces instead of or in addition to hydrodynamic focusing to position cells or particles in a flowing stream for analysis. Commercial implementations to date combine both hydrodynamic and acoustic focusing together to enable high precision analysis of a broad dynamic range of volumetric sample input rates up to an order of magnitude higher than is practical with hydrodynamic focus alone. This capability allows great flexibility in reducing assay time or modifying or eliminating concentration requirements or concentration steps in sample preparation protocols. It also provides a practical method for processing sub-microliter volumes using sample dilution. In order to take full advantage of this dynamic range, it is necessary to understand the fundamental benefits and limitations of acoustic focusing as applied to flow cytometry. © 2018 by John Wiley & Sons, Inc.

Keywords: acoustic focus • acoustic cytometry • high-speed flow cytometry • hydrodynamic focus • sample preparation

How to cite this article:
Ward, M. D., & Kaduchak, G. (2018). Fundamentals of Acoustic Cytometry. *Current Protocols in Cytometry*, *84*, e36. doi: 10.1002/cpcy.36

INTRODUCTION

Hydrodynamic focusing uses sheath flow to confine injected sample fluid to a small "sample core" that is typically accelerated to meters-per-second velocity through an optical interrogation region defined by a tightly focused laser beam. The first description of acoustic focusing applied in flow cytometry (Goddard et al. 2006) mimicked this process without requiring sheath flow by exploiting physical differences between cells or particles relative to the background carrier medium to position the particles or cells in a single, focused line along the central axis of a glass capillary. Subsequent commercially available acoustic focusing cytometers have combined hydrodynamic focusing and acoustic focusing together by applying the acoustic focus to a similar ultrasonic capillary device used to inject the sample into a sheath manifold (Acoustic Focusing Overview, 4/12/2017). By focusing cells into a tight line prior to injection in the sheath manifold, precise alignment of cells in interrogating lasers can be maintained at much higher volumetric inputs than possible with hydrodynamic focus alone (Figure 1). These higher input rates enable dilute samples to be processed quickly, without resorting to centrifugation or other concentration steps. Alternately, they allow dilution of concentrated samples or modifying of protocols for lower cell concentrations, without fear of long analysis times.

Acoustic cytometry as referred to herein uses acoustic radiation pressure to align cells in flow for analysis in an interrogation region using optical detectors. It should not be confused with flow cytometry that uses acoustic energy to interrogate cells, (Roos & Apfel, 1988) or that detects acoustic energy from the photoacoustic effect, which is stimulated by light pulses. (Galanzha & Zharov, 2012). Acoustic alignment could however be used together with acoustic interrogation, and detection and photoacoustic analysis has already been combined with acoustic alignment in vivo (Galanzha et.al., 2016).

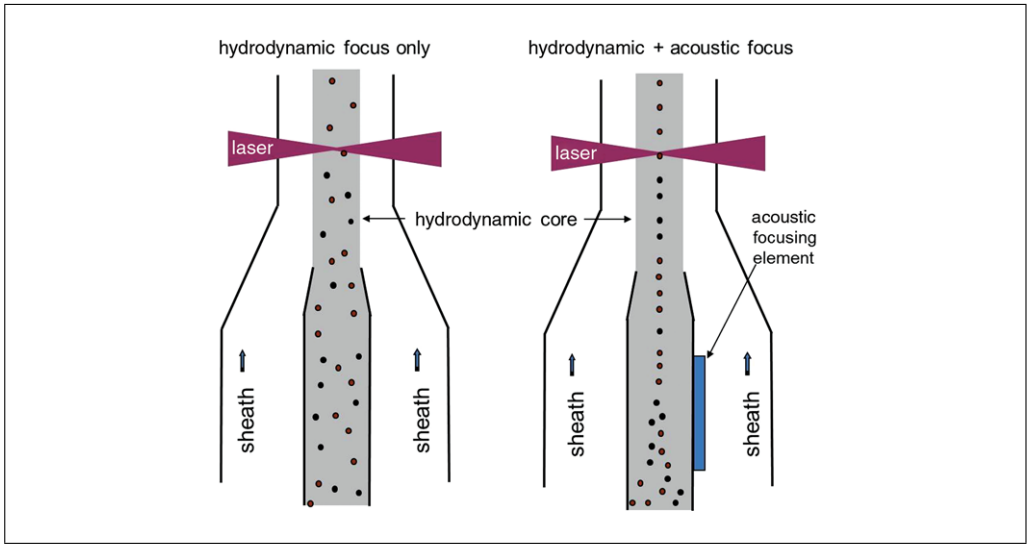

Figure 1 Comparison of hydrodynamic focus alone (left) versus Acoustic-assisted hydrodynamic focus (right) at a high volumetric sample input rate. Acoustic focusing of particles before sample injection into the sheath manifold allows velocity and illumination precision to be maintained for large sample cores resulting from these rates.

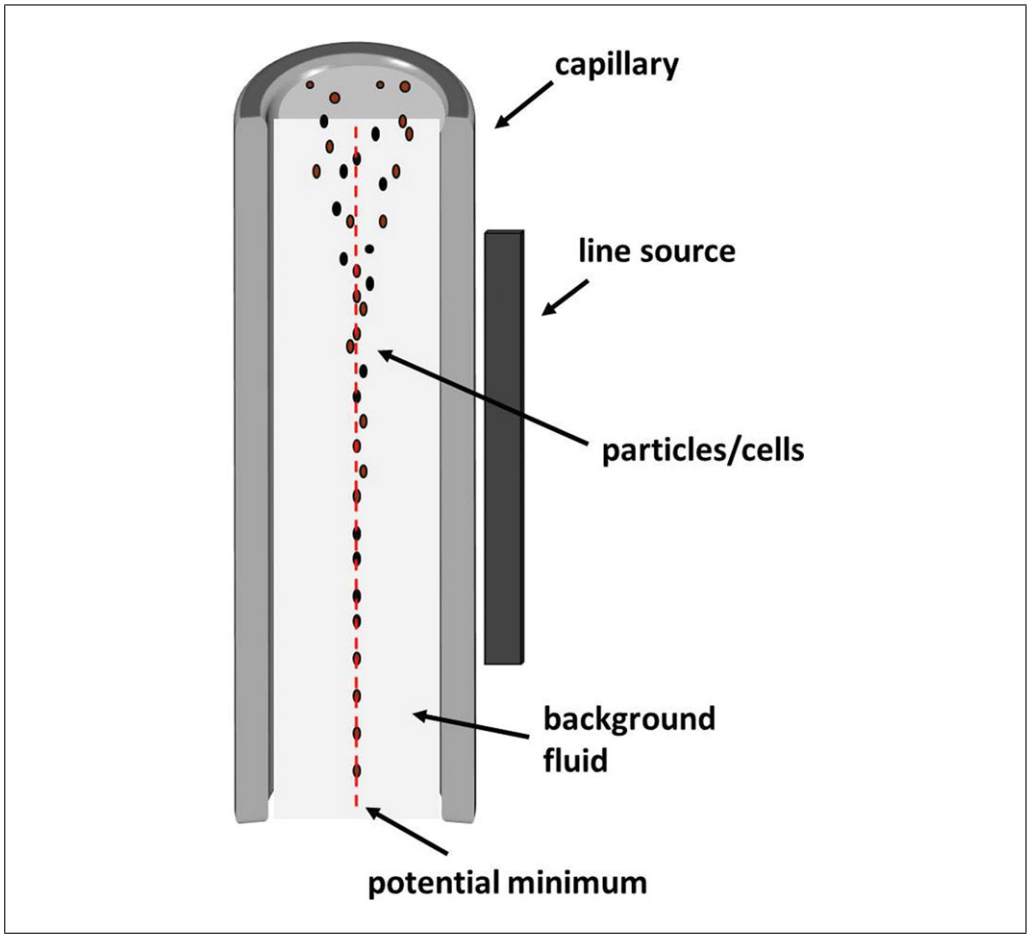

Figure 2 Schematic of a line-driven capillary depicting tight single line focusing of particles in a flowing liquid using acoustic radiation pressure.

The effect of acoustic radiation pressure on particles in a medium was first described by Kundt and Lehmann (1874) after they witnessed dust particles levitated in organ pipes. This effect has been applied to aqueous solutions for the separation of bioparticles (Coakley, Bardsley, Grundy, Zamani, & Clarke, 1989, 2000; Curtis & Stephans, 1982; Jönsson, Nilsson, Petersson, Allers, & Laurell, 2005; Yasuda, Haupt, & Unemura, 1997). Use of acoustic fields for separation of cells and or positioning cells for analysis continues to be an active area of research today, with wide ranging applications including bulk processing of algae for bio fuels and cells for cell therapy, multiple focused lines of cells for high throughput flow cytometry (Piyasena et al., 2012), and single cell manipulations like cell sorting (Ren et al., 2015). Ren et al. used acoustic traveling waves and a surface acoustic wave device or SAW to sort cells, but the bulk of these studies use resonant square or rectangular cavities to create acoustic standing waves. The acoustic cytometers described here use standing waves generated by a circular focusing device called a line-driven capillary. The line-driven capillary, described by Kaduchak et al. (2008), is an acoustically resonant device that focuses cells or particles into a single line using a capillary driven by a single piezoelectric transducer or line-source (Figure 2). The theory of this device is described by Goddard and Kaduchak (2005).

THE ACOUSTIC-ASSISTED HYDRODYNAMIC FOCUSING CYTOMETER

Commercial instruments employing these acoustic-focusing devices are more aptly named "acoustic-assisted hydrodynamic focusing cytometers" because they use the line-driven capillary to inject sample into a sheath manifold, in much the same way as a sample injection probe is used in a conventional cytometer (Figure 3).

In contrast, the first acoustic cytometer focused particles without sheath flow (Goddard, Martin, Graves, & Kaduchak, 2006). There are advantages to eliminating sheath, but practical challenges as well. In a sheathless cytometer, the sample is free to contact and contaminate optical flow cell walls. In addition, particle velocity, and therefore dwell time in an interrogating laser, is linearly dependent on volumetric sample input rate. A primary advantage of acoustic focus is that data precision can be maintained over a large dynamic range of volumetric sample input rates. However, in order to take advantage of this range without sheath flow, the electronics and software would need to accommodate

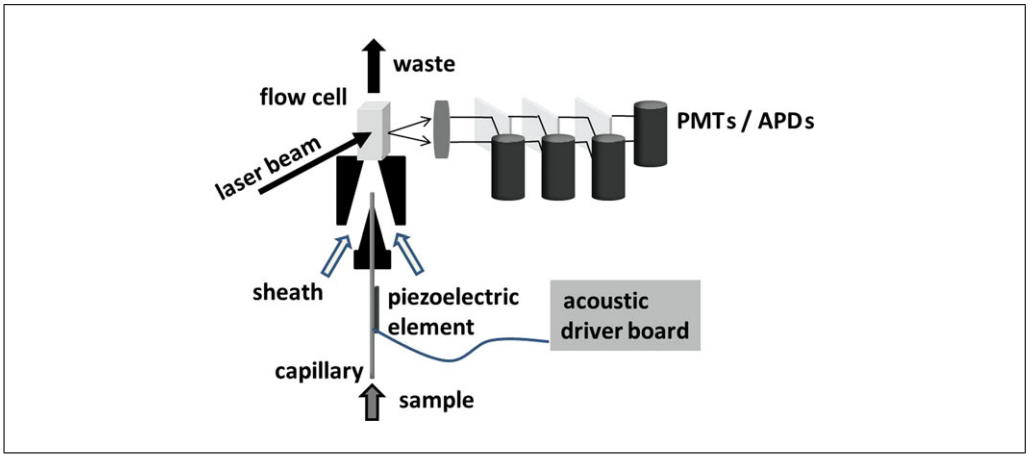

Figure 3 Generic illustration of an acoustic assisted hydrodynamic focusing analyzer. Sample is forced into the capillary, acoustically focused, injected into a sheath manifold, analyzed, and transferred to waste. As for a conventional flow cytometer, the analysis stage includes a laser beam focused at the position of the particles in the optical cell. The scatter/fluorescent signal is conditioned by appropriate optical filters before optical detection. Driving and control electronics are added to ensure the piezoelectric device is driven at the acoustic resonance frequency of the piezoelectric element/capillary.

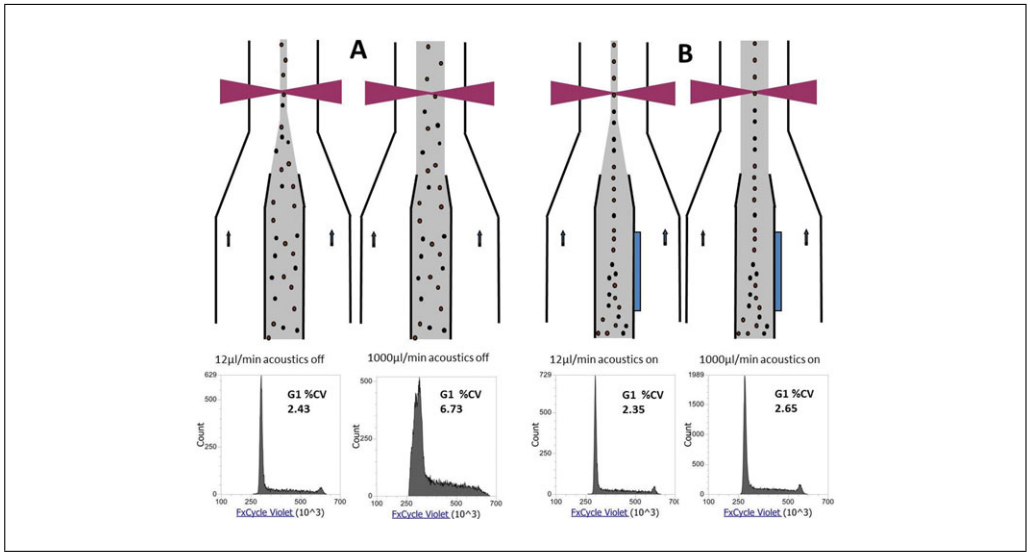

Figure 4 Schematic drawings of hydrodynamic focus only (**A**) and acoustic assisted hydrodynamic focus at low (left) and high (right) sample input rates. Directly under each schematic is a corresponding cell cycle histogram of FxCycle™ Violet area taken at low (12 µl/min) and high (1000 µl/min) flow rates.

signals across the same large dynamic range of velocities and laser dwell times. For the instrument used to collect the data presented in Figure 4, the flow rate spans nearly two orders of magnitude (12 µl/min to 1000 µl/min).

Apart from the acoustic capillary and its driving electronics, all the other components in Fig 3 could be used to construct a conventional cytometer. In fact, the instrument can be used as a hydrodynamic focus only instrument by simply turning off the acoustic driver board. This board drives the vibration of the line-driven capillary device using feedback control that ensures that the resonant frequency required for a tight focus is maintained. This frequency varies with the capillary diameter and wall thickness. A 300-µm inner diameter capillary, for example, may have a resonance near 3 MHz, whereas a 600-µm inner diameter capillary resonates at a proportionately lower frequency near 1.5 MHz. The resonance also varies with temperature and fluid properties. The variations for the range of temperatures and samples used in flow cytometry are relatively small, with resonant frequency changes on the order of a few percent, but the feedback control is still essential to ensure optimum performance over this entire range.

During operation of the cytometer, a discreet flow rate between 12 and 1000 µl/min is chosen and the instrument adjusts its sheath rate such that the ratio of sample to sheath is highest at the lowest rate and lowest at the highest rate. Figure 4 shows schematics for low and high sample input rates with acoustic focusing turned on or off. Cell cycle histograms for actively growing alcohol fixed and FxCycle™ Violet stained Jurkat cells are paired with each schematic. See supplementary material for protocol details. Figure 4A shows the two rates with the acoustic field off (hydrodynamic focus only). The 12 µl/min rate shows the good precision required for cell cycle analysis, whereas the 1000 µl/min rate precision is only useful for counting cells. With the acoustic field off, the cells are free to distribute across the large core, and signal precision is degraded by increased variation of cell velocity and illumination intensity of the laser. For this instrument, the precision drop due to illumination position variation is partly mitigated by a flat top laser beam profile, but the G1 cell cycle stage coefficient of variation (CV) is a high 6.73% and the G2 cell cycle peak disappears entirely. With the acoustic field turned on in Figure 4B, velocity and illumination intensity precision are high for both low and high rates. The CV benefit for the acoustic focus vs. no acoustic focus at 12 µl/min is small at 2.35%

versus 2.43%, respectively, because of the high ratio of sheath to sample at this rate. The precision benefit of acoustic focus tapers off with the decrease in sample core diameter, providing no additional benefit as the core diameter approaches the cell or particle size. In other words, acoustic focus does not push a 10 μm diameter cell any closer to the center of a 10 μm diameter sample core than does hydrodynamic focus.

The high precision demonstrated in Figure 4B at 1000 μl/min enables running of samples up to 10 times faster than in cytometers without acoustic focus. This does not mean, however, that all samples should be run this fast. Understanding how best to take advantage of this increased throughput can be made easier by answering the following questions: (1) How are different cells or particles focused by the acoustic field? (2) What is the acoustic concentration effect and how does it pertain to sample concentration and injection rates? Once these questions are answered, one can begin to ask about how acoustic cytometry can help answer questions in biology, chemistry, and medicine.

ACOUSTIC FORCE ON PARTICLES IN A MEDIUM

The answer to the question of how cells or particles are affected by acoustic focus starts with the mechanical properties of both the particles and the medium they are carried in. Equation 1 gives the acoustic force U exerted on a particle in a carrier medium, Gorkov (1962):

$$U = \frac{4}{3}\pi a^3 \left[\left(\beta_o \frac{\langle p^2 \rangle}{2} \right) f_1 - \frac{3}{2} \left(\frac{\rho_o \langle v^2 \rangle}{2} \right) f_2 \right]$$

Equation 1

Here, a is the particle radius, β_0 is the compressibility of the surrounding fluid, and ρ_0 is the density of the surrounding fluid. The pressure and velocity of the acoustic field in the absence of the particle are described by p and v, respectively, and the brackets correspond to a time-averaged quantity. The terms f_1 and f_2 are the contrast terms that determine how the mechanical properties (compressibility and density, respectively) of the particle differ from the background medium. They are given by the following Equations 2a and 2b:

$$f_1 = 1 - \frac{\beta_p}{\beta_o}$$

Equation 2a

$$f_2 = \frac{2\,(\rho_p - \rho_o)}{(2\rho_p + \rho_o)}$$

Equation 2b

The subscript p corresponds to intrinsic properties of the particle. The force F acting on a particle is related to the gradient of the force potential U by Equation 3:

$$F = -\nabla U$$

Equation 3

Particles will be localized at positions where the potential U displays a minimum (stable equilibrium). The acoustic contrast of a particle (or medium) is determined by the density and compressibility differences between it and the background medium as defined by terms $f1$ and $f2$ in Equations 2a and 2b. The relative magnitudes and signs of $f1$ and

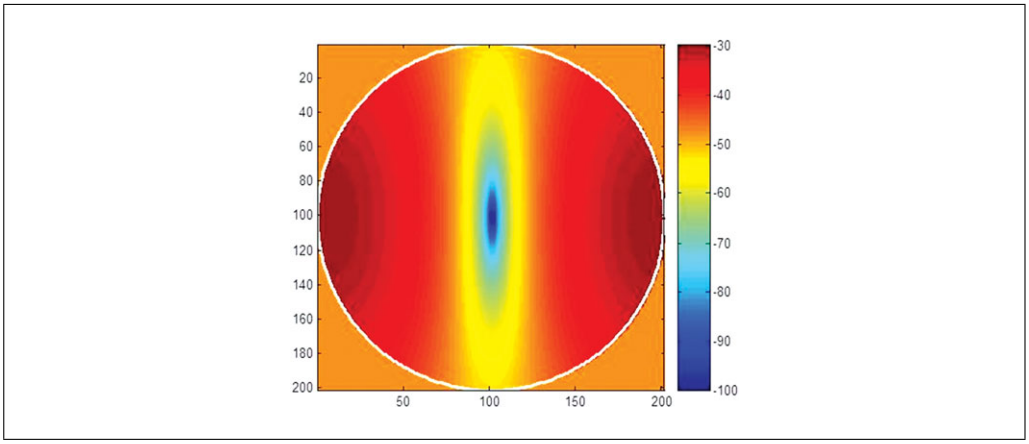

Figure 5 Calculated acoustic force potential in the cross-section of an acoustically driven capillary. Particles with positive acoustic contrast are focused toward the force potential trap in the center of the cross-section. Note that that the acoustic field is asymmetric, with stronger gradients along the axis of the piezo driver. This asymmetry can improve precision of analysis of non-spherical cells by helping to orient them in interrogating lasers.

$f2$ determine the behavior of the radiation force potential U and thus determine the magnitude and direction of the acoustic radiation pressure force. As an example, if a particle and the background medium share the same density value ($\rho p = \rho 0$), then $f2$ is zero and the acoustic contrast is due only to compressibility differences in $f1$. If both $f1$ and $f2$ are zero, then there is no acoustic contrast. Figure 5 displays the force potential U for an erythrocyte within the cross section of an acoustically driven capillary containing phosphate buffered saline. Particles traveling through the capillary experience a time averaged force that transports them into the deep potential well centered along the axis of the capillary.

It should be noted that nearly all particles and cells of interest have acoustic contrast values in water or aqueous buffers, which force them to migrate to the central axis of the capillary (as shown in Figure 5). These particles have positive acoustic contrast in theses fluids. There are a few materials such as fat particles and gas bubbles that have negative acoustic contrast which forces their migration toward the wall of the capillary in the acoustic field.

Effects on Cell Health and Viability

Detrimental acoustic effects on cells are invariably at the top of the list of concerns for many cell biologists when introduced to the topic of acoustic focusing. This is because ultrasonic energy is routinely used for lysis of cells as hardy as bacterial spores. Like most acoustic resonators designed for cell manipulation (Wiklund, 2012), line driven acoustic capillaries used for cytometry are different from devices designed to lyse cells in fundamentally important ways. First, acoustic lysis is typically done using sub-megahertz frequencies that can create cavitation, a phenomenon in which tiny gas bubbles form and collapse with tremendous local shear and heating. The acoustic focusing capillaries used here operate at a frequency well above 1 MHz without cavitation. Second, acoustic lysis is performed at very high energy levels where acoustic streaming and rapid fluid heating are common. Acoustic cytometry is performed with relatively low energy levels of tens of milliwatts maximum electrical input power at the high sample flow rate of a milliliter per minute. At lower flow rates, this power is progressively scaled down. The acoustic energy dissipated in the fluid is also significantly less than the electrical input energy. The design of the acoustically driven capillary spreads this energy over the entire length of the capillary and there is very little sample heating. Goddard, Sanders, Martin, Kaduchak, and Graves (2007) showed that the viability of Chinese hamster ovary (CHO) cells was

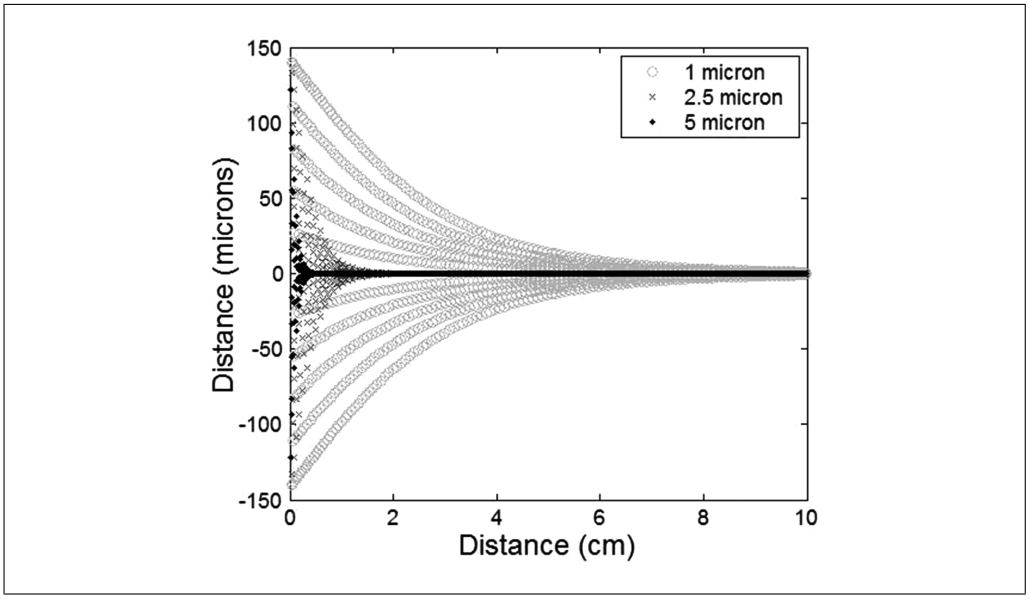

Figure 6 Calculated trajectories of different diameter microspheres as they travel along the axis of the acoustic focusing capillary. The vertical axis is the particle position relative to the capillary axis. The horizontal axis is the particle position along the length of the capillary. Sample flows from left to right at a rate of 1000 μl/min.

not significantly affected by the acoustic field created by a large acoustically driven capillary even in the sub-megahertz region. The higher, gentler megahertz frequencies now utilized in commercial cytometers are routinely used in safe medical imaging of patients and are thought to be gentle enough for cell separations where cell health or recovery are critical, such as cell therapy (FloDesign Sonics) or circulating tumor cell separation. (Li et al., 2015). Pre-focusing in the injector with acoustics also serves to reduce the acceleration of cells required in the subsequent hydrodynamic focus where cells can undergo significant shear forces.

Particle or Cell Size

While many cells and microbes have similar acoustic contrast, the acoustic force on different sized particles varies widely. As can be seen from Equation 1, the acoustic force is proportional to the third power of the particles' radius. The force resisting movement of the particle is the Stokes drag force F_d, which can be approximated by the following Equation 4 for a hard sphere with particle Reynolds numbers <0.1:

$$\mathrm{F_d} = 6\pi r_p \eta_{\mathrm{ur}}$$

Equation 4

Here r_p is the cell or particle radius, η is the medium viscosity, and u_r is the acoustically induced velocity in the radial direction. F_d is linearly proportional to radius, so the net result is that overall force is proportional to the particles' radius squared with small particles moving more slowly than large particles of similar acoustic contrast. Figure 6 shows the predicted trajectories of various sizes of polystyrene beads in a sample flowing in the axial direction in the acoustic capillary. As can be seen from this figure, it takes longer for the smaller particles to reach the capillary axis. This in turn dictates that volumetric sample throughput should be reduced when processing smaller particles such as bacteria. If the residence time within the capillary of particles or cells of a given size is not long enough, the variation in position of the particles/cells about the central capillary axis will be greater and the coefficient of variation (CV) of the optical measurement will

suffer at the higher sample input rates. Acoustics may contribute to focus and may also align asymmetric cells but smaller particles should generally be analyzed at conventional sample input rates, so that the additional hydrodynamic focusing can help ensure higher precision.

If the particle is so small that the acoustic force is weaker than Brownian motion, the acoustic field will not have a focusing effect, such that positioning precision will depend solely on the hydrodynamic focus. This size cutoff is a function of acoustic contrast factors, acoustic power, and frequency and is beyond the scope of this unit, but in general, nano particles, like exosomes and viruses, should be analyzed with low sample input rates/high sheath to sample ratios, as in any flow cytometer.

THE ACOUSTIC CONCENTRATION EFFECT

The focusing of all cells in the capillary volume to a line in the center of the capillary creates a local effective cell concentration that can be many times higher than the initial starting concentration. This enables much faster analysis of dilute samples, but it necessitates the addition of sheath fluid at higher cell concentrations in order to maintain single particle analysis. Figure 7 illustrates the acoustic concentration effect in the absence of sheath. Whole blood diluted to about 2×10^7 (Figure 7A and B) and 2×10^6 red blood cells per ml (Figure 7C) was imaged in a quartz flow cell after pumping through a capillary with the acoustic field turned off (7A) and on (7.B and C). When the acoustic field is on, all of the positive acoustic contrast particles in the capillary are forced to the center before being pumped into the flow cell. This effect in relatively concentrated samples results in a rope-like sheet of particles that can be many particles in width like that seen in Figure 7B.

In the instrument, this rope is injected into a sheath manifold where sheath fluid speeds up and separates the cells, creating single particle spacing dependent on the sample to sheath ratio. A 1:10 sample to sheath ratio for example, would create spacing similar to that seen in the 10-fold dilution of sheathless sample in Figure 7.C. Rope-like conditions similar to Figure 7B can be created in the laser interrogation zone of the instrument itself by diluting less and running at high sample input rates. For a 10-fold dilution of blood

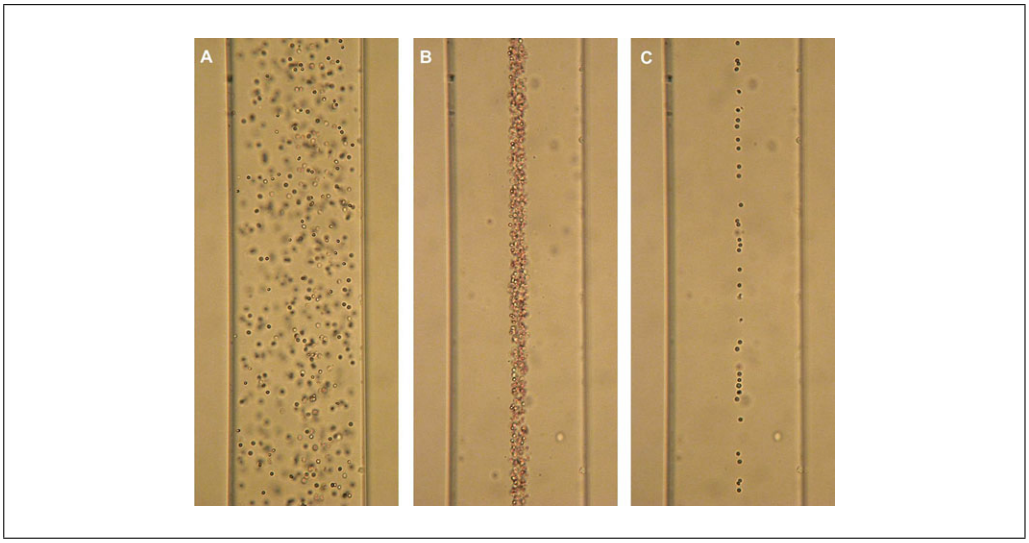

Figure 7 Micrographs of dilute acoustically focused whole blood pumped into in a square quartz flow cell without sheath. (**A, B**) 2×10^7 RBCs per ml (**C**) 2×10^6 RBCs per ml. In the instrument, where sheath flow accelerates the sample and separates the cells, a 100 fold and a 10 fold higher concentration respectively run at 1000 µl /min would be needed to produce similar concentrations to B and C in the laser interrogation zone.

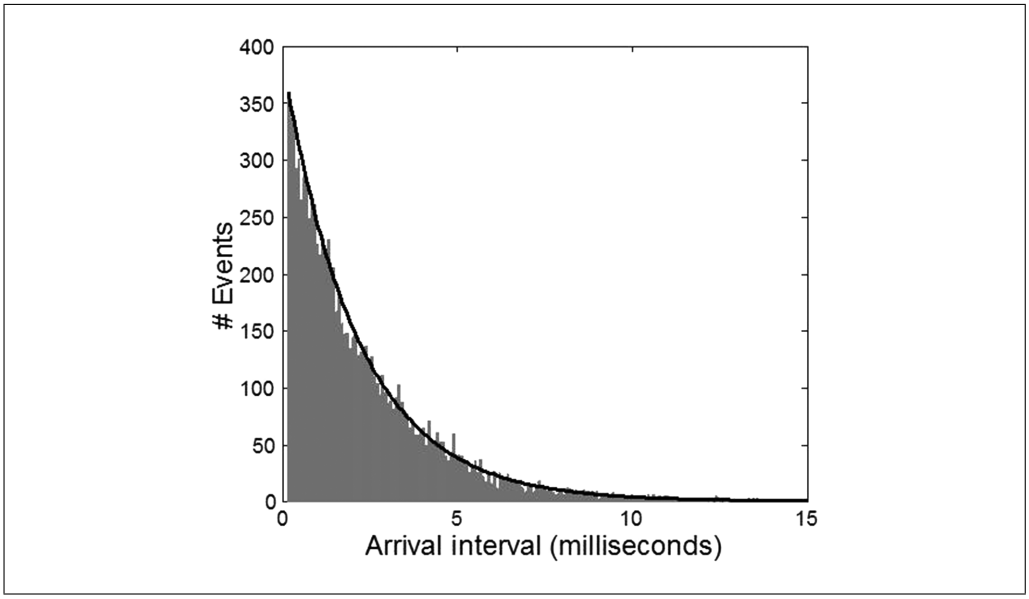

Figure 8 Plot of number of events versus arrival interval at the interrogation laser for acoustically focused microspheres in flow at 1 ml/min without sheath flow. The black line is an exponential distribution. The experimental data (gray bars) closely matches this prediction.

containing 5×10^9 RBCs per ml and injected at 1000 µl/min, approximately 8 million RBCs per second pass through the instrument. For a core velocity of 8 meters/second, this averages about 10 cells per 10 micron length of sample core. With several cells in the laser focus at all times, scatter is completely useless, but fluorescence data can still be collected from white blood cells. This sounds attractive from a throughput standpoint, because white blood cell coincidence under these conditions is still relatively rare for whole blood, but the quality of fluorescence data is degraded. Higher concentration of unbound fluorophore, combined with non-specific staining, reduces sensitivity such that this technique can typically only be used for high density antigens with bright labels. An additional effect is the absorbance of violet laser light by hemoglobin, which further diminishes signals for violet excitable probes.

Volumetric Throughput, Poisson Rate and Coincidence

Although acoustic cytometers can process sample volumes an order of magnitude faster than conventional cytometers, this does not mean that all samples should be processed this fast. This is often desirable for more dilute samples, but at higher concentrations, all cytometers, including acoustic ones with or without sheath, are limited by coincident events as governed by Poisson statistics. Figure 8 shows that the inter-arrival times of particles that have been acoustically focused follow an exponential distribution, which is in agreement with a Poisson process.

Poisson statistics predict the likelihood of one cell, no cells, or more than one cell being present in an event window. As sample throughput increases with higher sample concentration, the probability of a cell being present in an interrogating laser beam in any given window of time increases, but the probability of more than one cell being present in the laser also increases (a coincident event).

Coincidence in an event window should generally be kept low by using mean rates of less than one event per ten event windows for most assays (van den Engh, 2000). This condition theoretically corresponds to a 10% coincidence rate. While speed of electronics can also limit event rates, most modern cytometers are capable of electronic event rates

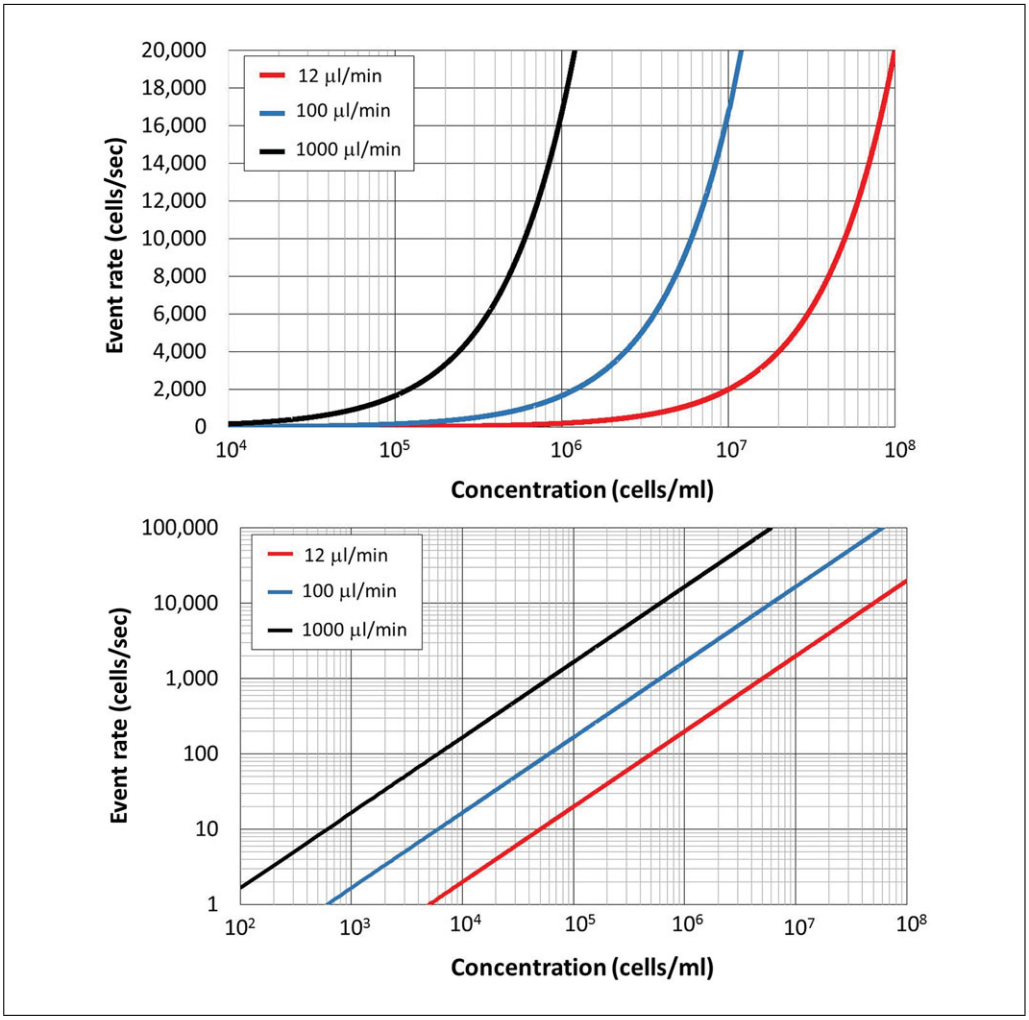

Figure 9 Linear versus log (top) and log versus log (bottom) plots for cell event rate versus initial sample concentration for sample input rates of 12, 100, and 1000 µl/min. Event rates are theoretical and exclude the impact of coincidence. Linear plotting of event rate emphasizes the low event rates obtained with cell concentrations below one million per milliliter at conventional rates. Log plotting of event rate shows both the need for high throughput rates at the lowest cell concentrations and the danger of exceeding maximum instrument event rates at high cell concentrations.

that significantly exceed their 10% Poisson rate, which is governed by the magnitude and variation of cell velocity.

Large variation in cell velocity for large sample cores limits sample core size and consequently volumetric throughput in a conventional cytometer. The size of an event window dictates the Poisson rate, and in a cytometer with spatially separated lasers, the event window must typically be extended to account for different laser to laser arrival times for particles or cells having different velocities. In a large core without acoustic focus, the large spread in transit times requires larger event windows which decrease the Poisson rate.

If lower coincidence is desired or higher coincidence is acceptable, sample concentration and or volumetric sample rate should be adjusted accordingly with a corresponding decrease or increase in particle throughput. Figure 9 shows linear (top) and log (bottom) plots of theoretical event rates that exclude the impact of coincidence. Event rates are in cells per second as a function of the log of sample concentration for three different volumetric flow rates: 12, 100, and 1000 µl/min. The first two rates cover a similar

dynamic range to most conventional cytometers and the third is the highest rate on the acoustic cytometer. Many flow cytometry protocols are written for cell concentrations in the millions per milliliter range. The plots show that this is no accident, since this is where the event rate for the first two traditional sample input rates reaches the hundreds and low thousands per second, where analysis time can be kept reasonable while maintaining lower coincidence.

The linear versus log plot emphasizes that much below one million cells per milliliter, conventional sample rates can mean long analysis times. At 100,000 cells per milliliter a 100 μl/min input rate delivers just 167 cells per second and the 12 μl/min rate delivers only 20 per second. The log versus log plot gives a quick look at extremely low concentrations, where event rates dip below 1 cell per second at concentrations less than 600 and 5000 cells per milliliter for these flow rates respectively. At the high concentration extremes, the log versus log plot readily shows that the high acoustic assisted sample input rate of 1000 μl/min can easily deliver cells fast enough to exceed instrument Poisson rates above concentrations of one million cells per ml. This rate of 35,000 events/sec for the instrument used here, is reached for a concentration of just over two million cells per milliliter. It follows then, that for many conventional cytometry protocol concentrations, a lower sample rate should be used or the sample should be diluted.

A DIFFERENT PARADIGM FOR SAMPLE DILUTION

With acoustic focus, the additional order of magnitude for the sample throughput rate that is possible, allows cytometrists to think outside the box of conventional sample protocol concentrations. Sample dilution is often kept to a minimum in cytometry protocols because of fear of long analysis times, but dilution need not be feared with the higher volumetric throughput. The high dynamic range of the acoustic assisted cytometer offers great flexibility in reducing assay time, reducing assay concentration requirements or eliminating concentration steps. Dilute samples can be run quickly and samples that are diluted during sample preparation protocols may sometimes be run without an otherwise needed final centrifugation step.

Protocols may also be altered if there is a benefit to lower concentration such as reduced cell sticking. Some sample preparation protocols, like magnetic bead separations for example, can have higher purity and/or recovery when the final separation step in the magnetic field is performed with greater dilution. Higher dilutions are often not used however, as losses in any additional required concentration step offset these benefits.

A less obvious benefit of dilution is that it allows a greater percentage of cells to be analyzed without fear of sucking up an entire sample and introducing air into the system. Assuming an instrument dead volume and a residual volume that is typically left in a tube after processing, the percentage of cells left behind is linearly related to the dilution factor. If for example 50 μl of a concentrated 100-μl sample are left after analysis, this translates to 50% unanalyzed cells. If the same sample is diluted 10-fold before analysis, only 5% of the cells will remain in the same 50 μl residual volume.

Small initial sample size

High volumetric sample throughput combined with high dilution factors make it practical to use very small initial sample sizes without fear of losing significant cells to instrument dead volume or residual volume. Even fractions of very small samples can often be used for experimental set-up or alternate sample treatments.

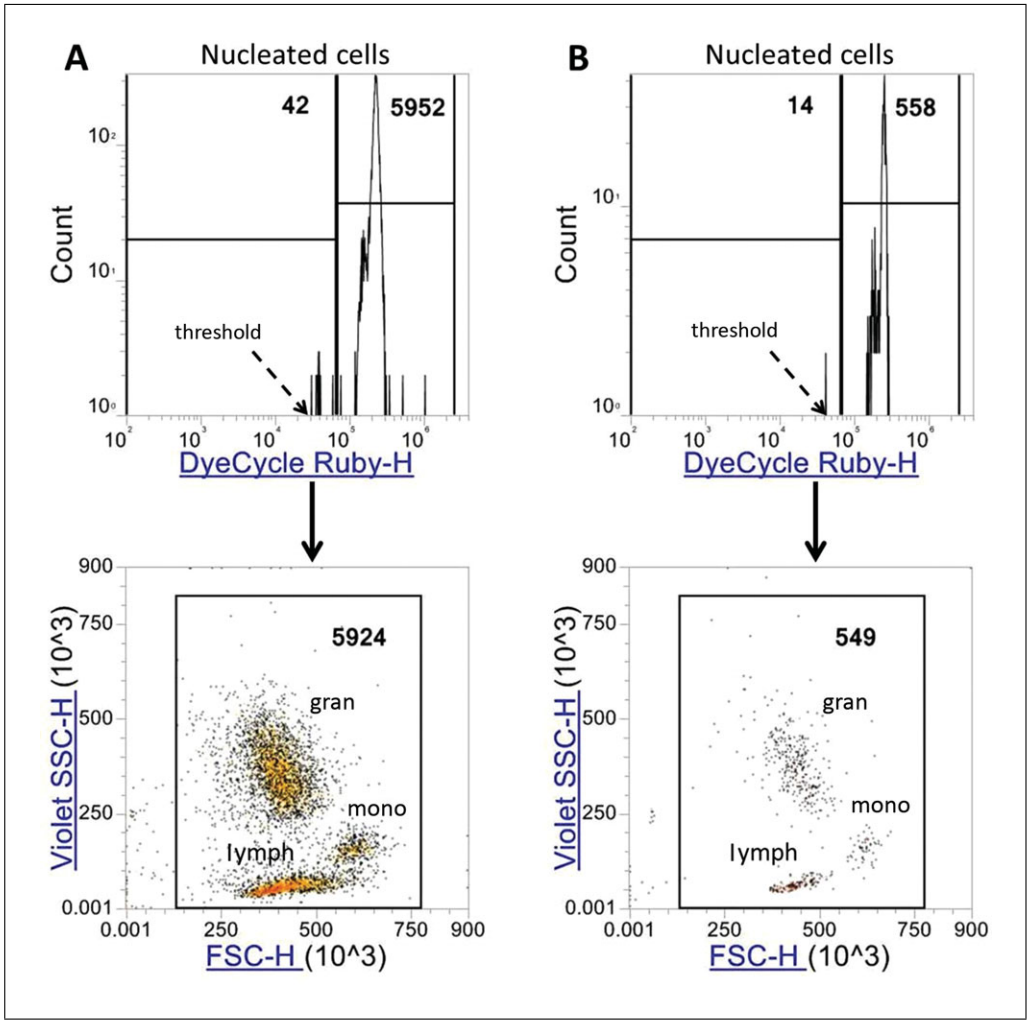

Figure 10 Analysis of nucleated cells from 940 nl (**A**) and 94 nl (**B**) of whole blood with 850-fold and 8500-fold dilution, respectively. Nucleated cells are plotted on a log log histogram of DyeCycle™Ruby fluorescence showing the threshold level used for collection and a linear 405 nm violet SSC-H versus FSC-H differential scatter plot showing white blood cell populations Granulocytes (Gran), Monocytes (Mono), and Lymphocytes (Lymph).

For precious samples where analyzing every cell is important, combining a "no lyse, no wash" protocol with high dilution prevents cell loss from centrifugation or lysis reagents and decreases cells lost in residual volume. For Figure 10A a 1 µl sample of whole blood was diluted into 850 µl of DyeCycle™Ruby nucleic acid staining buffer and 800 µl, of this dilution was run at 1000 µl/min with an analysis time of about 46 sec. For Figure 10B, the 1 µl sample is diluted as for A and 85 µl of this dilution was diluted another 10-fold and run as in A. Nucleated cell events are captured by thresholding on DyeCycle Ruby high events.

For each sample, 800 µl of an 850 µl sample or 94% of the sample is analyzed, equating to 940 nl (A) and 94 nl (B) of the original whole blood sample. Each sample is plotted with a log log histogram of DyeCycle Ruby fluorescence and a corresponding differential white blood cell scatter plot using 405 nm violet SSC-H versus FSC-H (488 nm blue). For full protocol and instrument setup, see supplementary material. Note that for whole unlysed blood on this instrument, the position of granulocytes in FSC is shifted significantly to the left relative to ammonium chloride lysed blood. Red blood cell lysis protocols can change white blood cell morphology, particularly for granulocytes. The differences in FSC seen from morphology changes are dependent on interrogating light parameters

including wavelength, scatter collection angles and laser focus and alignment. (Petriz et al., 2017).

For "no-lyse, no-wash" protocols and for any protocol in which a wash step may be removed, it is important to understand how assay background can either be increased by the large sample cores generated at high volumetric input rates or reduced by dilution of the free fluorophore in a sample.

Background reduction from dilution

One concern that arises when proposing elimination or significant reduction of sheath ratios is that the benefit of squeezing the sample core to a very small size, such that very little free fluorophore is excited by the laser, is lost. If the sample core is large, the laser will excite free fluorophores throughout the beam focus, resulting in higher background for unwashed samples. This effect is mitigated somewhat by the tight Gaussian focus of the laser beam and by spatial filtration in the collection optics, but for a given concentration of unbound fluorophore, fluorescence background is higher than for a tightly hydrodynamically focused core. With dilution, however, the concentration of free label is reduced by the dilution factor, reducing the fluorescence background. Dilution, like washing by centrifugation, will disturb the binding equilibrium, but for higher affinity labels, dissociation will be insignificant if it is performed within a reasonable time before analysis. For many antibodies with useful affinity, dissociation half-lives are on the order of hours or days. If dissociation for lower affinity ligands is of concern, rapid dilution followed by analysis with a high volumetric sample rate can be used as a quicker alternative to centrifugation for background reduction.

As a frame of reference for background reduction, a single round of centrifugation, depending on operator and dilution prior to and after centrifugation, is typically comparable to about a 300-fold dilution. For a properly titrated immunophenotyping experiment with high affinity antibodies, non-specific binding contributes more to background than does unbound fluorophore at this dilution, and continued dilution beyond 500 to 800-fold may not significantly reduce background levels.

Note that for lower affinity reagents like nucleic acid stains, dilution can disturb equilibrium in a short period of time and that for some high precision assays like cell cycle analysis, the dilution buffer should contain equilibrium concentrations of these low affinity stains. This can increase background in large cores, even for dyes considered "non-fluorescent" until bound, depending on the dye concentration and the ratio of fluorescence enhancement upon binding.

SUMMARY AND OUTLOOK

Use of acoustic fields for separation and positioning of cells and particles has been an active and growing area of research for nearly four decades. Diverse uses of these fields in flow cytometry have been suggested, including pre-analysis sample preparation, acoustic cell sorting, multi-stream analysis and sheathless triggered stopped or even reverse flow analysis. Commercial implementations to date have focused on combining sheath and acoustic focusing to create instruments capable of high precision analysis over a high dynamic range of volumetric sample inputs from 12 μl/min to 1000 μl/min.

This expansion of dynamic range enables up to an order of magnitude faster analysis times versus conventional hydrodynamic focusing alone, particularly for dilute samples, and provides greater flexibility in sample preparation protocols. Protocols can be modified to run lower concentrations of cells, eliminate extra concentration steps or dilute to extend the number of experiments possible or increase the percentage of cells analyzed in very small volumes. Flexibility for sample dilution ratios is particularly useful for optimization

of no lyse no wash assays where red blood cell lysis and centrifugation are avoided to minimize potential sample preparation artifacts.

Increasing availability of more and more parameters in flow cytometry has spurred discovery of new cell types, more correlation of phenotyping with live cell function and increasing scrutiny of smaller and smaller phenotypic and functional cell subpopulations. The concern that sample preparation causes loss or alteration of specific fragile cells has grown in the face of this research, making protocols that can minimize impact on live cells and their response to environment and stimuli highly desirable.

Understanding the fundamental advantages and limitations of acoustic focusing as applied to flow cytometry can enable users to better leverage the technology, not only to increase throughput and save time but also to modify and improve sample preparation and minimize its effects on cell biology.

Acknowledgements

The authors thank Marc DeJohn of Biomeme Inc. and the late Carl Stewart and Patrick Turner for their significant contributions to the implementation of acoustic focusing in flow cytometry. We also thank Jolene Bradford of Thermo Fisher Scientific for valuable support and advice.

Conflicts of Interest

The authors are employees of Thermo Fisher Scientific, which is in the business of selling flow cytometers and flow cytometry reagents.

Literature Cited

Acoustic Focusing Overview, 4/12/(2017). Retrieved from https://www.thermofisher.com/us/en/home/life-science/cell-analysis/flow-cytometry/flow-cytometers/acoustic-focusing-technology-overview.html. Accessed November *28*, 2017.

Coakley, W. T., Bardsley, D. W., Grundy, M. A., Zamani, F., & Clarke, D. J. (1989). Cell manipulation in ultrasonic standing wave fields. *Journal of Chemical Technology and Biotechnology*, *44*, 43–62. doi: 10.1002/jctb.280440106.

Coakley, W. T., Hawkes, J. J., Sobanski, M. A., Cousins, C. M., & Spengler, J. (2000). Analytical scale ultrasonic standing wave manipulation of cells and microparticles. *Ultrasonics*, *38*, 638–641. doi: 10.1016/S0041-624X(99)00151-1.

Curtis, H. W., & Stephans, E. J. (1982). Ultrasonic continuous flow plasmapheresis separator. *IBM Technical Disclosure Bulletin*, *25*(1).

Galanzha, E. I., & Zharov, V. P. (2012). Photoacoustic flow cytometry. *Methods (San Diego, Calif.)*, *57*(3), 280–296. doi: 10.1016/j.ymeth.2012.06.009.

Galanzha, E. I., Viegas, M. G., Malinsky, T. I., Melerzanov, A. V., Juratli, M. A., Sarimollaoglu, M., ... Zharov, V. P. (2016). In vivo acoustic and photoacoustic focusing of circulating cells. *Scientific Reports*, *6*, 21531. doi: 10.1038/srep21531.

Goddard, G., & Kaduchak, G. (2005). Ultrasonic particle concentration in a line-driven cylindrical tube. *Journal of the Acoustical Society of America*, *117*, 3440–3447. doi: 10.1121/1.1904405.

Goddard, G., Martin, J. C., Graves, S. W., & Kaduchak, G. (2006). Ultrasonic particle concentration for sheathless focusing of particles for analysis in a flow cytometer. *Cytometry*, *69*, 66–74. doi: 10.1002/cyto.a.20205.

Goddard, G. R., Sanders, C. K., Martin, J. C., Kaduchak, G., & Graves, S. W. (2007). Analytical performance of an ultrasonic particle focusing flow cytometer. *Analytical Chemistry*, *79*, 8740–8746. doi: 10.1021/ac071402t.

Gorkov, L. P. (1962). Forces acting on a small particle in an acoustic field within an ideal fluid. *Soviet Physics-Doklady*, *6*, 773–775.

Jönsson, H., Nilsson, A., Petersson, F., Allers, M., & Laurell, T. (2005). Particle separation using ultrasound can be used with human shed mediastinal blood. *Perfusion*, *20*, 39–43. doi: 10.1191/0267659105pf782oa.

Kaduchak, G., Goddard, G., Salzman, G., Sinha, D., Martin, J. C., Kwiatkowski, C. S., & Graves, S. W. (2008). Ultrasonic Particle Concentration and Application in Flow Cytometry. *United States Patent*, *7*, 340, 957.

Kundt, A., & Lehmann, O. (1874). Longitudinal vibrations and acoustic figures in cylindrical columns of liquids. *Annalen der Physik und Chemie (Poggendorff 's Annalen)*, *153*, 1–11.

Li, P., Mao, Z., Peng, Z., Zhou, L., Chen, Y., Huang, P-H., ... Huang, T. J. (2015). Acoustic separation of circulating tumor cells. *Proceedings of the National Academy of Sciences of the United States of America*, *112*(16), 4970–4975. doi: 10.1073/pnas.1504484112.

Petriz, J., Bradford, J. A., & Ward, M. D. (2017). No lyse no wash flow cytometry for maximizing minimal sample preparation.

Methods (San Diego, Calif.), pii, S1046–2023(17)30159–30157. https://doi.org/10.1016/j.ymeth.2017.12.012.

Piyasena, M. E., Suthanthiraraj, P. P. A., Applegate, R. W. Jr., Goumas, A. M., Woods, T. A., López, G. P., & Graves, S. W. (2012). Multinode Acoustic Focusing for Parallel Flow Cytometry. *Analytical Chemistry*, *84*, 1831–1839. doi: 10.1021/ac200963n.

Ren, L., Chen, Y., Lia, P., Maoa, Z., Huanga, P.-H., Rufoa, J., ... Huang, T. J. (2015). A high-throughput standing surface acoustic wave (SSAW)-based cell sorter. *Lab on A Chip*, *15*(19), 3870–3879. doi: 10.1039/C5LC00706B.

Roos, M. S., & Apfel, R. E. (1988). Application of 30-MHz acoustic scattering to the study of human red blood cells. *Journal of the Acoustical Society of America*, *83*, 1639–1644. doi: 10.1121/1.395918.

van den Engh, G. (2000). High speed cell sorting. *In Emerging Tools for Single-Cell Analysis: Advances in Optical Measurement Technologies* (pp. 21–48). G. Durack, & J. P. Robinson (Eds.), New York: John Wiley and Sons.

Wiklund, M. (2012). Acoustofluidics 12: Biocompatibility and cell viability in microfluidic acoustic resonators. *Lab on A Chip*, *12*, 2018–2028.doi: 10.1039/c2lc40201g.

Yasuda, K., Haupt, S. S., & Unemura, S. (1997). Using acoustic radiation force as a concentration method for erythrocytes. *The Journal of the Acoustical Society of America*, *102*, 642–645. doi: 10.1121/1.421009.